Challenges and Successes when Generating In-Season Multi-Temporal Calibrated Aerial Imagery

Josh Pritsolas[1], Randy Pearson[1], Jensen Connor[2], and Peter Kyveryga[2]

Southern Illinois University Edwardsville[1]
Department of Geography
Laboratory of Applied Spatial Analysis
Edwardsville, IL 62026

Iowa Soybean Association
Analytics[2]
Ankeny, IA 50023

A paper from the Proceedings of the
13th International Conference on Precision Agriculture
July 31 – August 4, 2016
St. Louis, Missouri, USA

Abstract. *Digital aerial imagery (DAI) of the crop canopy collected by aircraft and unmanned aerial vehicles is the yardstick of precision agriculture. However, the quantitative use of this imagery is often limited by its variable characteristics, low quality, and lack of radiometric calibration. To increase the quality and utility of using DAI in crop management, it is important to evaluate and address these limitations of DAI. Even though there have been improvements in spatial resolution and ease of imagery access, current DAI sources appear to lack the end-user demand for products that provide more than just an aesthetic image of a place-specific snapshot at a given time. The objective of this study was to establish a site to test quality and different methods for radiometric calibration of DAI over time. A 120-ha study area located in Story County, Iowa was used during the 2015 growing season. Commercial calibration tarps with known reflectance (3, 6, 12, 22, 44, and 56%) values were deployed in a study area with two fields of corn (Zea mays L.) and two fields of soybean (Glycine max L.). Two commercial DAI providers collected 0.2 meter and 0.5 meter, multi-spectral (blue, green, red, and NIR) digital imagery every 10 to 12 days throughout the growing*

season. Empirical line method and segmental linear regression calibration techniques were utilized to convert digital numbers (DNs) to percent reflectance, which were used to create standardized NDVIs that could be compared across time (date to date) and across space (field to field). Image processing challenges resulted from a highly non-linear mathematical relationship between DN values and percent reflectance, and from significant inaccuracies in the spatial registration of pixels from flight to flight. Even so, calibrated temporal vegetation indices were produced allowing for identification of agronomic areas that had similar vegetative health over time. The analyses showed that it is critical for DAI providers to maintain the purest form of the original digital values (with minimal post-processing manipulation) to allow for radiometric calibration of the data for use in spatiotemporal vegetation indices, crop modeling, and any other standardized image comparisons for use in crop management.

Keywords. *Remote sensing, digital aerial imagery, radiometric calibration, vegetation indices, NDVI, and crop management.*

INTRODUCTION

The applications of remote sensing in agriculture is well documented, from the identification of stem rust in wheat (Keegan et al., 1956) and the assessment of corn leaf blight by Bower et al. (1971) to crop identification and crop yield forecasting (Anuta and MacDonald, 1971; Gardner et al., 1985). Yet, even with these early successes in the application of remote sensing to agriculture, the last twenty-five years has seen limited acceptance by the agricultural community to wholly embrace the technology. Pearson et al. (1994) identified three potential impediments to the widespread acceptance of remote sensing applications in agriculture during these early years. These impediments were: 1) the ability to collect and deliver remotely sensed data with a high frequency, 2) the ability to rapidly disseminate the processed data, and 3) the ability to calibrate the data so that it could be compared from field to field (across space) and from one date to the next (across time).

In the last twenty years, technological advances in imaging systems and web-based delivery systems have all but wiped two of these impediments from our collective memories. The ability to collect digital aerial imagery (DAI) (from both aircraft and drones) on a weekly basis, or even a daily basis, is now almost commonplace. And, the ability of DAI providers to disseminate the collected data to the end-user within hours of acquisition is considered the norm in the industry. Yet it is the third impediment that still seems to be plaguing the industry—image calibration that allows spatial and temporal comparisons of remotely sensed imagery. This calibration process is especially important as the agricultural industry moves toward a more prolific use and understanding of vegetation indices (Hatfield et al., 2008), such as the NDVI (Deering, 1978; Tucker, 1979) and its various modifications (Huete, 1988; Qi et al., 1994). In order to make these indices truly meaningful, data must be converted from raw digital numbers (DNs) to percent reflectance.

While methods of calibrating aerial imagery were published over two decades ago (Richardson et al., 1991; Pearson et al., 1994) the industry has been slow to move toward the acceptance of any calibration process, and, in many cases seems to be ignoring it all together. With that said, the research in this study takes a new look at the calibration process (and the resulting vegetation indices) of DAI through the use of ground-based commercial calibration tarps.

RADIOMETRIC CALIBRATION REVIEW

When one reviews the current literature associated with remote sensing and DAI as a practical application in agriculture, three themes immediately emerge: 1) the use of vegetation indices, 2) the use of imagery products for crop management, and 3) utilization of radiometric calibration techniques for remotely sensed data. These three themes are essential to the processes that enable DAI to aid end-users in developing methods to monitor crop health and crops stress. However, it must be noted that the first theme (and to a large degree the second theme) is heavily reliant on the third theme: that of radiometric calibration. Therefore, it is this theme (radiometric calibration of imagery) on which this study will focus. A review of the literature yielded two types of radiometric calibration techniques, which attempt to account for illumination and atmospheric effects (Smith and Milton, 1999). The first was normalization or image averaging and the second was the empirical relationship between radiance and reflectance.

Normalization

Normalization of data is often nothing more that manipulation of a digital image so that all data uses the same scale or data range. This normalization process can be achieved in a variety of ways including the use of data stretching techniques and the use of the soil line. While not truly calibrated, data (when normalized) can often be compared spatially and temporally. A good example of this normalization process was implemented in a recent study by Kyveryga et al. (2012). The researchers in this study employed a normalization process by using uncalibrated DAI, but implemented normalization by extending the dynamic range of DAI so that 80% of the pixel values were within ±2 standard deviations of the mean DN. The normalization method used in that study provided adequate results at a feasible cost (because of extensive size of the study area), as opposed to costly ground-based techniques that often require some sort of ground control.

Empirical Line Method of Calibration

The empirical line method for calibrating DAI is defined as the linear relationship that exists between the DNs and corresponding ground targets that have a known percent reflectance within the field of view (FOV) of an image, thus eliminating any sensor or atmospheric influence (Smith and Milton, 1999). Several studies have used the empirical line method with varying mathematical techniques being employed to obtain the calibrated relationship between DN values and reflectance (Pearson et al., 1994; Speckman et al., 2000; Shanahan et al., 2001; Fitzgerald et al., 2003; Markelin et al., 2008; Zhang et al., 2009; Clemens, 2012). Moreover, by gathering percent reflectance values from known targets (with the understanding that an adequate number of targets and an adequate range of reflectance values are used), radiometric calibration can be accurate with an error of only a percent or two, which can produce reliable and acceptable results (Smith and Milton, 1999). Following this notion, many of the studies previously mentioned implemented the empirical line method with small variations on the underlying concept. One study employed the use of a spectroradiometer to gather percent reflectance from static ground targets for calibration (Zhang et al., 2009). Several other studies used placards constructed as Richardson et al. (1991) described (Pearson et al., 1994; Speckman et al., 2000) or a form of a white reflectance panel (Clemens, 2012). However, the majority of the more recent studies have employed various numbers of tarps with known percent reflectance for the conversion of DNs to percent reflectance. (Shanahan et al., 2001; Fitzgerald et al., 2003; Markelin et al., 2008).

STUDY OBJECTIVES

While there is a great deal of literature on the various vegetation indices and the uses of imagery products for crop management, it is important to realize that the first step in truly understanding the

value of remote sensing in agriculture is to understand the significance and utility of calibrated versus uncalibrated imagery. It was also evident when reviewing the literature that much of the intricacies of calibration techniques (from the various studies) were generalized without much detail provided to outline the specifics used for the methodology. With this being stated, the emphasis of this preliminary research with Iowa Soybean Association (ISA) was to focus on a comprehensive investigation of radiometric calibration techniques using percent reflectance tarps with implementation of the empirical line method (and regression analysis) to develop a model for generating temporally comparable NDVIs. This research was conducted using two independent image providers that collected imagery across the growing season on a 10 to 12-day cycle (weather permitting). The ultimate goal of this study was to determine and report on the complexities involved in, and the issues surrounding the generation of, the development of radiometrically calibrated data for use in various vegetation indices.

STUDY SITE, MATERIALS, AND DATA PROVIDERS

Farm Field in Story County, Iowa

The remote sensing study site used in this research was a corn (*Zea mays* L.) -soybean (*Glycine max* L.) rotational farm field in Story County, Iowa (Figure 1). This site also contained areas of perennial vegetation, roads, and buildings. The study area was approximately 120-ha in size and consisted of multiple fields of corn and soybean, various soil types, and rolling elevations ranging from 290-315 meters above sea level.

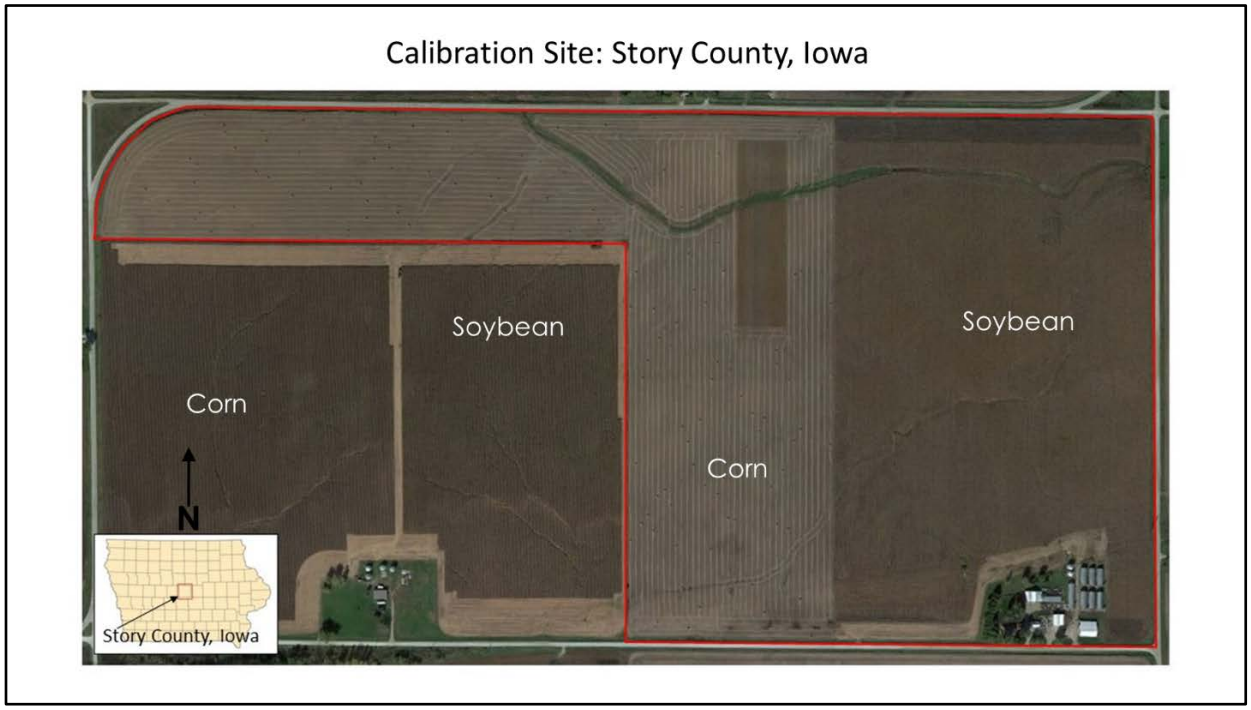

Figure 1. Layout reference of remote sensing study site, outlined in red. Data was also provided for the two fields not outlined in red.

Tarp Materials

The tarps deployed throughout the growing season of 2015 were purchased from Group VIII Technology (G8T) (Provo, UT) (Figure 2). The first set of tarps purchased were 6, 12, 22, and 44% reflectance and the second set purchased were 3 and 56% reflectance. Manuals with charts of the

percent reflectance and the raw data from these readings were provided for all six tarps (Figure 3). These tarps were all 3x3 meters in size and were the Type-822 fabric of moderate weight woven polyester substrate (G8T, 2015a; 2015b). All G8T tarps displayed a Lambertian quality and contained small-blackened brass eyelets that could be overlapped during deployment to create a gray scale display by staking them to the ground in an open area (2015a; 2015b).

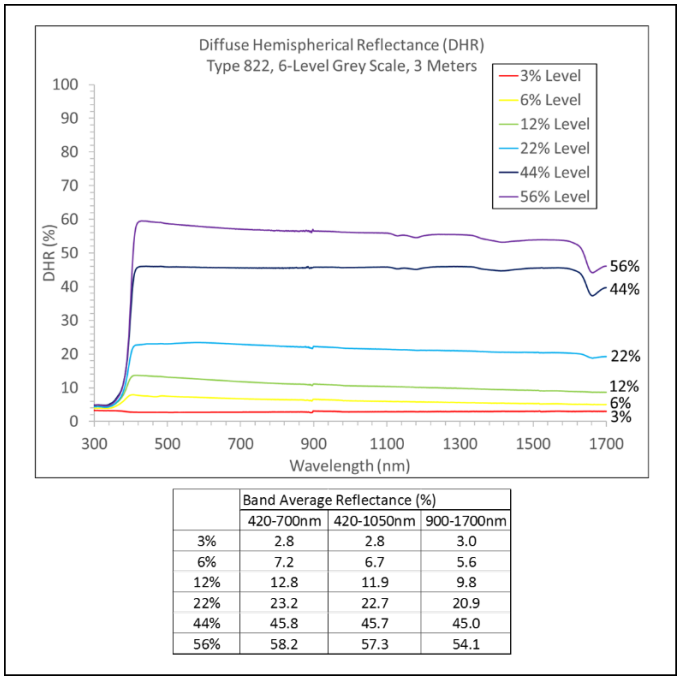

	Band Average Reflectance (%)		
	420-700nm	420-1050nm	900-1700nm
3%	2.8	2.8	3.0
6%	7.2	6.7	5.6
12%	12.8	11.9	9.8
22%	23.2	22.7	20.9
44%	45.8	45.7	45.0
56%	58.2	57.3	54.1

Figure 2 (left). All six tarps in gray scale array deployed before an August 27th, 2015 flight. From background to foreground: 3, 6, 12, 22, 44, and 56% reflectance (Photo by Dr. Randy Pearson). Figure 3 (right). Spectral curve for 3, 6, 12, 22, 44, and 56% reflectance tarps with band averages. Figure 3 was generated with raw data provided by G8T (2015a; 2015b).

DAI Providers

There were two digital aerial imagery providers (DAI-P) for the 2015 growing season. The names of the image providers are being withheld from this study and will be referred to as DAI-P1 and DAI-P2. First, DAI-P1 provided data throughout the growing season from May to September. DAI-P1 delivered a single file that was a 4-band image (blue, green, red, and NIR) that was rescaled from 12-bit data to 8-bit. The data provided were also a mosaicked and georeferenced image that covered the entire study area. Images were collected at a variety of times of the day throughout the growing season, ranging from early morning to mid-day. The system characteristics and product delivery specifications for DAI-P1 system were as follows: 1) bandwidths for blue (410-490nm), green (510-590nm), red (610-690nm), and NIR (800-900nm), 2) a spatial accuracy of ±3 meters, 3) images would be cloud and cloud-shadow free, and 4) the spatial resolution was set at 0.5 meters.

The DAI-P2 acquired data from June through September of the 2015 growing season. DAI-P2 delivered their data as two different files types. The first was a 3-band color image (blue, green, and red) that was collected at 16-bit and rescaled to 8-bit. The data were mosaicked and georeferenced to cover the entire study area. The second file contained a 3-band color infrared image (green, red, and NIR) that maintained the numeric integrity of the original imagery that was collected at 16-bit. These images were not mosaicked or georeferenced to any coordinate system. Like DAI-P1, data was collected at a variety of times of the day throughout the growing season, ranging from early morning to mid-day. The spatial resolution for all imagery from DAI-P2 was set at 0.2 meters.

Both DAI providers collected imagery throughout the growing season on the average of every 10 to 12 days. The goal for image capture was to have both providers collect imagery on the same day, or within a couple days of each other. Table 1 gives a breakdown of the DAI acquisition dates (and generalized time of day) along with available percent reflectance tarps.

Table 1. A general breakdown of dates and time of DAI capture from each provider with tarps present.

DAI-P1		DAI-P2	
Date Captured	Tarps Present	Date Captured	Tarps Present
May 21, mid-day	None		
June 9, mid-day	None	June 13, mid-day	6/12/22/44%
June 16, early morning	6/12/22/44%	June 17, late morning	6/12/22/44%
June 30, mid-day	6/12/22/44%		
July 12, late morning	6/12/22/44%	July 15, late morning	6/12/22/44%
July 31, mid-day	6/12/22/44%	July 30, mid-day	6/12/22/44%
August 15, early morning	6/12/22/44%	August 16, late morning	6/12/22/44%
September 1, mid-day	3/6/12/22/44/56%	August 27, late morning	3/6/12/22/44/56%
September 3, mid-day	3/6/12/22/44/56%		
September 12, late morning	3/6/12/22/44/56%	September 16, early morning	3/6/12/22/44/56%

CALIBRATION PROCESS

The calibration process utilized a variety of tools and techniques to convert each image band from DN values to percent reflectance. These processes included the collection or extraction of DN values from each tarp of each band for all images, the computation of mathematical models to convert DNs to percent reflectance for each band, and the processing of the full images through these mathematical models to generate calibrated imagery in support of NDVI generation.

Collection of DNs

The calibration process began with collecting DNs from the various reflectance tarp pixels located within each image. The tarp's DN values were collected using a 3x3-pixel matrix around the tarp's centroid. From the 3x3-pixel matrix, a DN value was selected from each reflectance tarp in each band of every image. For this study, the red and NIR DN values (and their corresponding percent reflectance) were arranged in a scatter plot to test for linearity. The DN collection process was accomplished by using ERDAS Imagine 2015™ (Hexagon Geospatial, Norcross, GA) and the scatter plots and best-fit regression lines were generated using Microsoft Office Excel 2015™ (Microsoft, Redmond, WA). It is important to mention that a low-end percent reflectance was calculated at 2% with the associated DN values located in shadowy dark areas (Moran et al., 2003; Beisl, 2012). This was necessary to increase the range of known percent reflectance anchors in the visible bands.

Computation of Mathematical Calibration Models

The computation of mathematical models to convert DNs to percent reflectance were calculated in Microsoft Excel™ through the use of a scatter plot and the addition of a best-fit trendline. Figure 4 shows the scatter plots and best-fit trendlines (red DNs plotted against corresponding percent reflectance) for both DAI providers for the June 16/17th images. Note that the relationship between DNs and percent reflectance for DAI-P1's red band was extremely non-linear and behaved in an exponential manner. For the red band, the 44% tarp was not used in the best-fit trendline because its corresponding DN had saturated at 255. This non-linear relationship was consistent for all images collected by DAI-P1. Conversely, the relationship between DNs and percent reflectance for DAI-P2's red band was highly linear with the trendline tracking through virtually every point (with $R^2 > 0.992$ for all images).

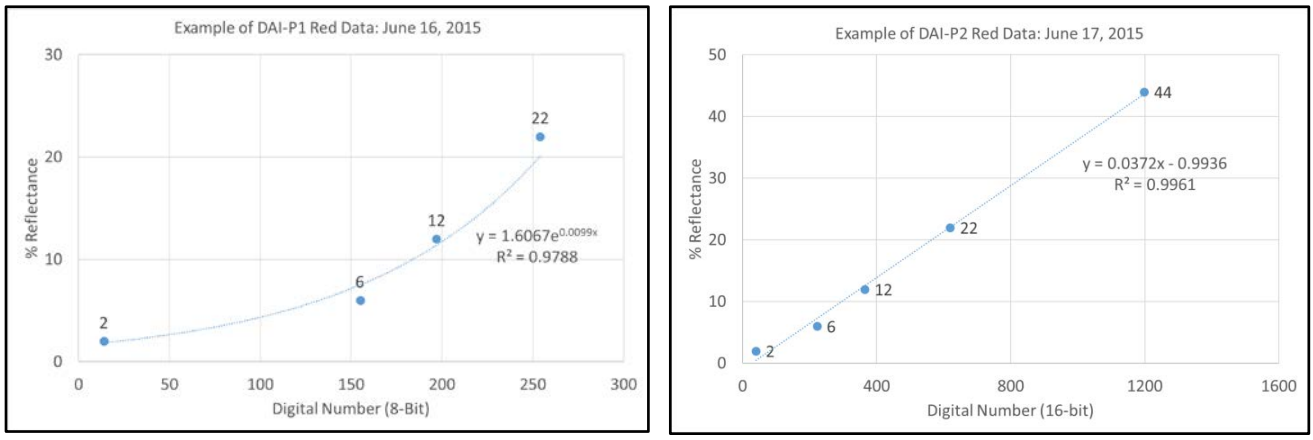

Figure 4. DAI-P1 (left) red band with non-linear exponential pattern. DAI-P2 (right) red band with linear relationship.

The relationship between DN's and percent reflectance for DAI-P1's NIR band was also extremely non-linear, but exhibited more of a logarithmic pattern (Figure 5). As with the red band, DAI-P2's NIR band exhibited this relationship for all images. However, the relationship between the NIR DNs and percent reflectance was (once again) highly linear for all DAI-P2 images with all R^2 values exceeding 0.987.

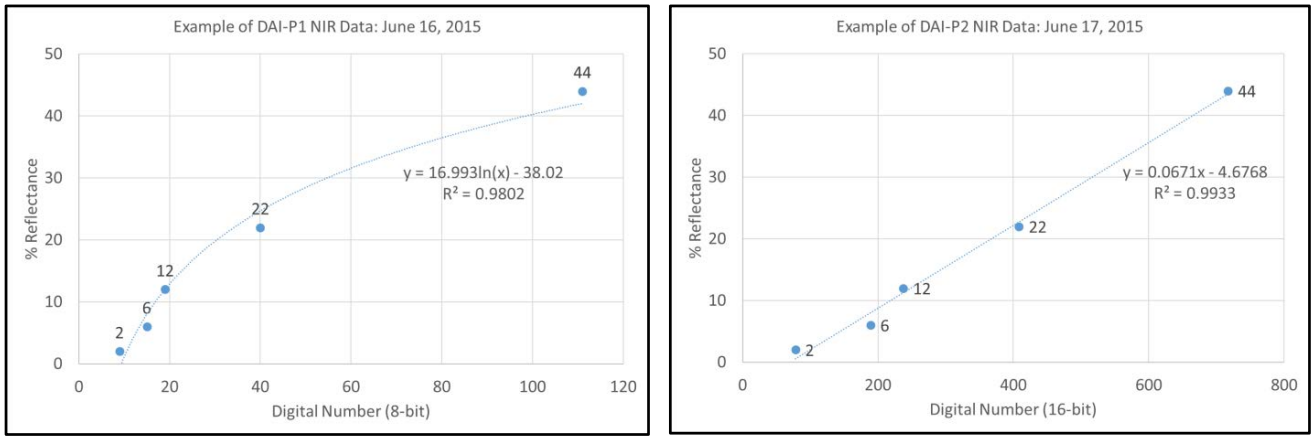

Figure 5. DAI-P1 (left) NIR band with non-linear near-logarithmic pattern. DAI-P2 (right) NIR band with linear relationship.

While the non-linearity of DAI-P2's red band and NIR band appeared exponential and logarithmic, respectively, the strength of these relationships was less than optimal for this project. Therefore, segmental linear regression was utilized as the best possible method for interpolation and extrapolation of predicted data values between and outside the range of known values. Segmental regression simply calculates a linear equation between increasing pairs of points (i.e., 2 to 6%, 6 to 12%, 12 to 22%, and so on). By utilizing the known percent reflectance values as breakpoints, linear regression was used between breakpoints to generate prediction equations (Figures 6). This method was outlined and used by Oosterbaan et al. (1990).

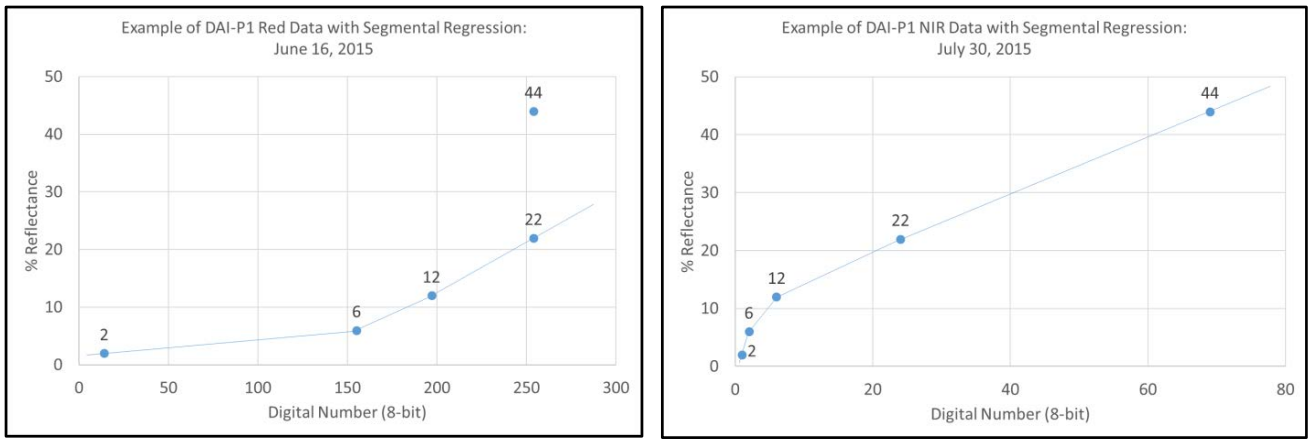

Figure 6. Examples of segmental linear regression fit to the breakpoints of DAI-P1 red (left) and NIR (right) bands.

When investigating the histograms of the DAI-P1 data it became apparent that the 6% tarp in the red band and the 44% tarp in the NIR band were not sufficient to provide the range needed to bracket the data distribution in the DAI and subsequently predict percent reflectance values. The histogram of the red data (Figure 7), along with an overlay of percent reflectance values, indicated that 94.1% of the digital data for the red band had no "tarp control" below 6% reflectance. This is especially important for vegetation analysis, since the red band's percent reflectance (at full canopy) was typically down in the 3 to 4% range. As well, the NIR band was limited on the high end with the 44% tarp (Figure 7). On July 31st, the crops in this study had 82.5% of the data with a NIR reflectance above 44%. Once this was noticed, two additional tarps were immediately purchased; a 3% tarp and a 56% tarp. This was not necessarily an issue in DAI-P2's data, since it was highly linear. However, there were potentially serious implications for DAI-P1's data because of its non-linearity.

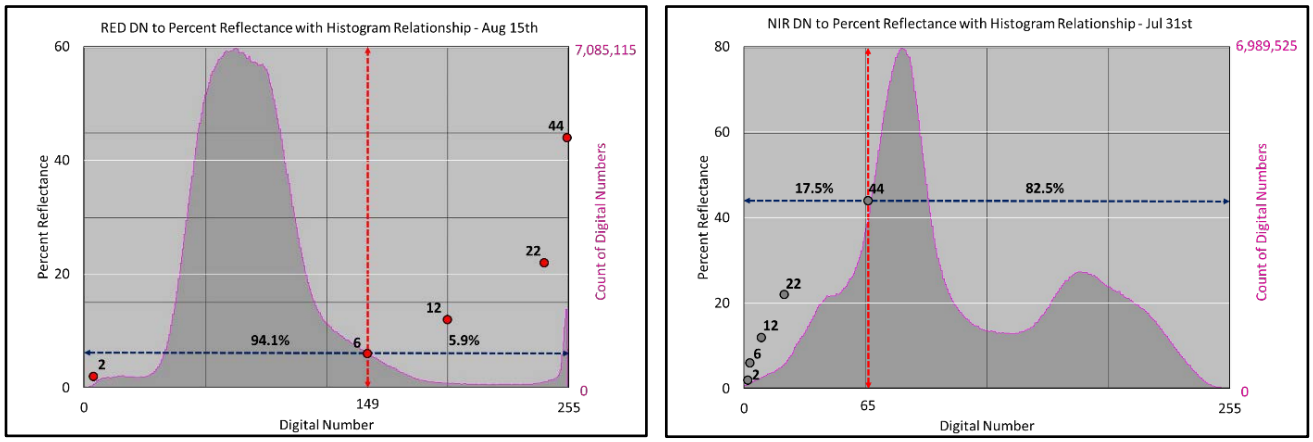

Figure 7. Examples of DN histograms for red (left) and NIR (right) data from DAI-P1. Plotted along with the histograms are the associated known percent reflectance values in relation to their positions along the histograms.

As mentioned earlier in this paper, the only DAI provider that delivered a fully mosaicked and georeferenced data set throughout the season was DAI-P1. Therefore, it was this dataset that was chosen as the base imagery to test and implement the calibration process for this study. However, this data set was more difficult to calibrate because of its non-linearity. In light of the fact that this study began without the proper range of reflectance tarps to address highly non-linear data, a workaround was developed to provide low red reflectance "pseudo calibration" targets and high NIR reflectance "pseudo calibration" targets. This was accomplished by georeferencing and overlaying

the DAI-P2's calibrated color infrared 16-bit image panels (nearest neighbor resampling) with the DAI-P1 geocorrected imagery (green, red, and NIR bands). Once overlaid, DN's from small polygons of DAI-P1 imagery could be related to the percent reflectance values of the same areas located within DAI-P2's calibrated imagery (flown on a similar date). This process allowed for the identification of numerous non-tarp calibration areas that could be used to refine the non-linear calibration equations for DAI-P1's data.

The graphs in Figure 8 show the linearity of DAI-P2's data with all six calibration tarps and the 2% shadow point. This linearity was exhibited in the last two flight acquired by DAI-P2 in which all six tarps were deployed. As well, the graphs in Figure 9 emphasizes the need for the additional 3% and 56% calibration tarps (and "pseudo calibration targets") to generate the most reliable calibration equations possible to address the non-linearity of DAI-P1's data. Additionally, an assessment of the "pseudo calibration targets" was conducted on multiple images across the season to determine the validity of the process. It was found that once DAI-P2's images were converted into percent reflectance using a simple linear model, small isolated areas from within the agricultural fields (of the calibrated images) could be used as surrogate targets for generating reliable calibration points for DAI-P1's images.

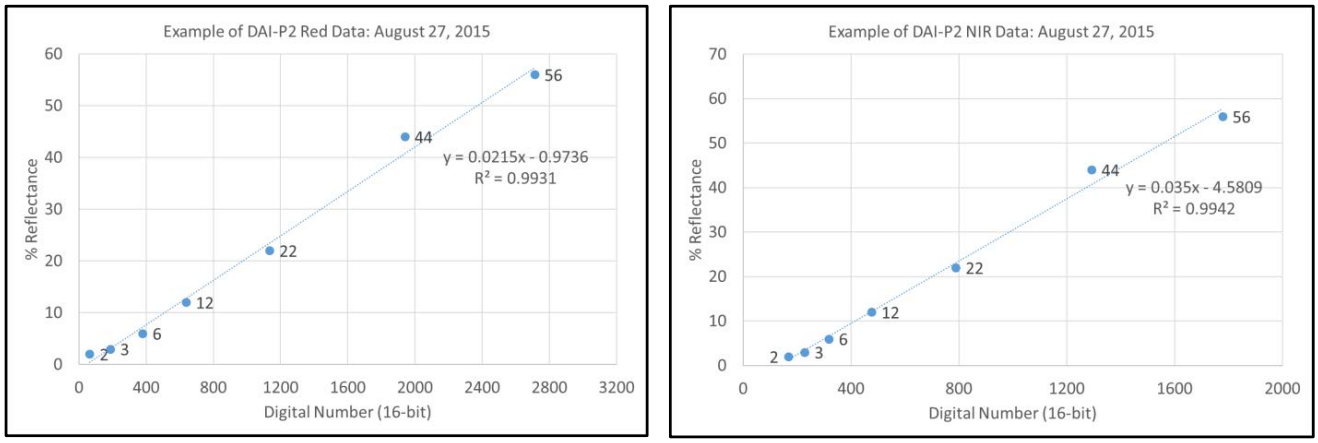

Figure 8. DAI-P2 red (left) and NIR (right) bands with linear data.

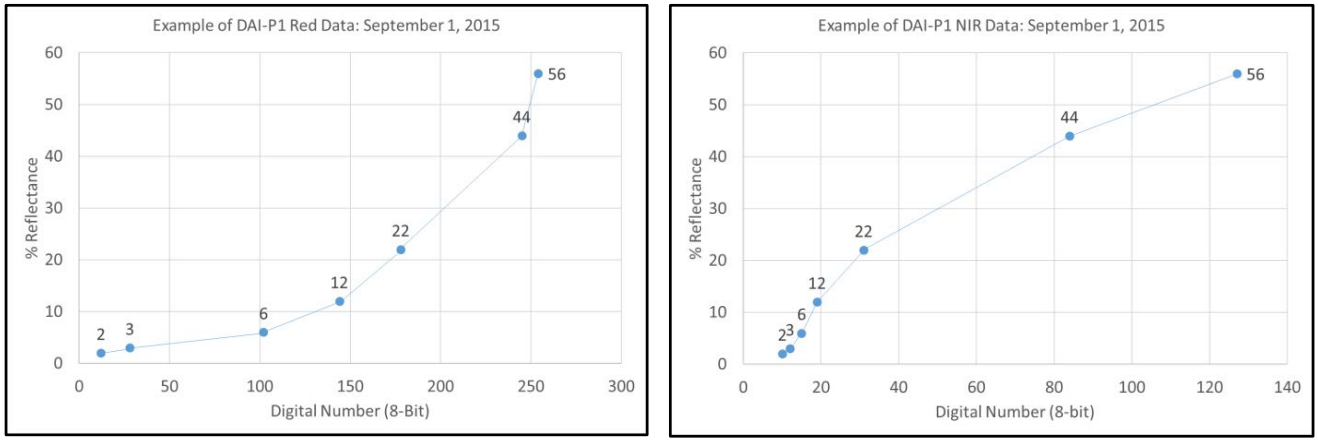

Figure 9. DAI-P1 red (left) and NIR (right) non-linear bands with segmental regression.

Calibration of Imagery and Computation of NDVIs

The actual conversion of the raw DNs from each image into percent reflectance utilized ERDAS Imagine's™ Spatial Modeler. This module of ERDAS™ enables the input of raw DNs from various

bands, the conversion of these bands into percent reflectance using the segmental regression equations, and finally, the computation of various vegetation indices as the final output. This entire process was developed into an actual model that allowed efficient picking of calibration points, the plotting of these DNs against percent reflectance values, the visual assessment of the scatter plot and the resulting segmental equations, the conversion of the DNs into percent reflectance, and finally the production of the calibrated NDVI.

COMPARRISON OF NDVI TEMPORAL SEQUENCES USING CALIBRATED AND UNCALIBRATED DATA

Once the calibrated NDVIs were computed they were stacked into a multi-layer file for temporal comparison. Figure 10 shows the location of 2 corn locations and 4 soybean locations in which the NDVI values were plotted over time (Figure 11). These plots used an Adjusted Relative Julian date starting on June 9th, 2015. The curves in Figure 11 are plots of each point's NDVI over time and are color coded to match the data points in Figure 10. An analysis of Figure 11 reveals several items of interest that should be noted.

1. There is a significant difference in the NDVI value of the four soybean plots on Day 1 of the chart (June 9th). Soybean 2 and Soybean 3 had significantly higher NDVI values than did Soybean 1 and the Soybean area that exhibited Sudden Death Syndrome (SDS) later in the season.
2. The two corn locations on Day 1 had significantly higher NDVI values that all soybean locations on the same date.
3. On Day 8 there was a significant increase in the NDVI in both corn and soybean.
4. On Day 20 (following a 4+ inch rainfall) the NDVI values for the sites with the least canopy closure (Soybean 1, Soybean 3, and Soybean SDS) had a significant lowering of their NDVI value. The lack of canopy closure allowed the sensor system to see through the thin and open canopy resulting in a significant influence from the wet bare soil. Soybean 2 on the eastern flank of the field and the two corn locations had enough biomass and canopy closure to mitigate the effect of soil moisture on the NDVI.
5. As is typical of NDVI (because of its use of the red band) there is a saturation or stagnation of the NDVI in the soybean fields around 0.88 to 0.92 (from Day 40 to around Day 70). During this time, one can see only subtle differences between Soybean 1, Soybean 2, and Soybean 3 points.
6. At Day 50, one can begin to see a decrease in the NDVI of the soybeans with SDS and the two corn locations.
7. Following Day 70, there is a significant divergence for all soybeans with Soybean 1 and Soybean 3 maintaining the highest overall NDVI. Soybean 1 and Soybean 3 areas had the highest yields that were reported.

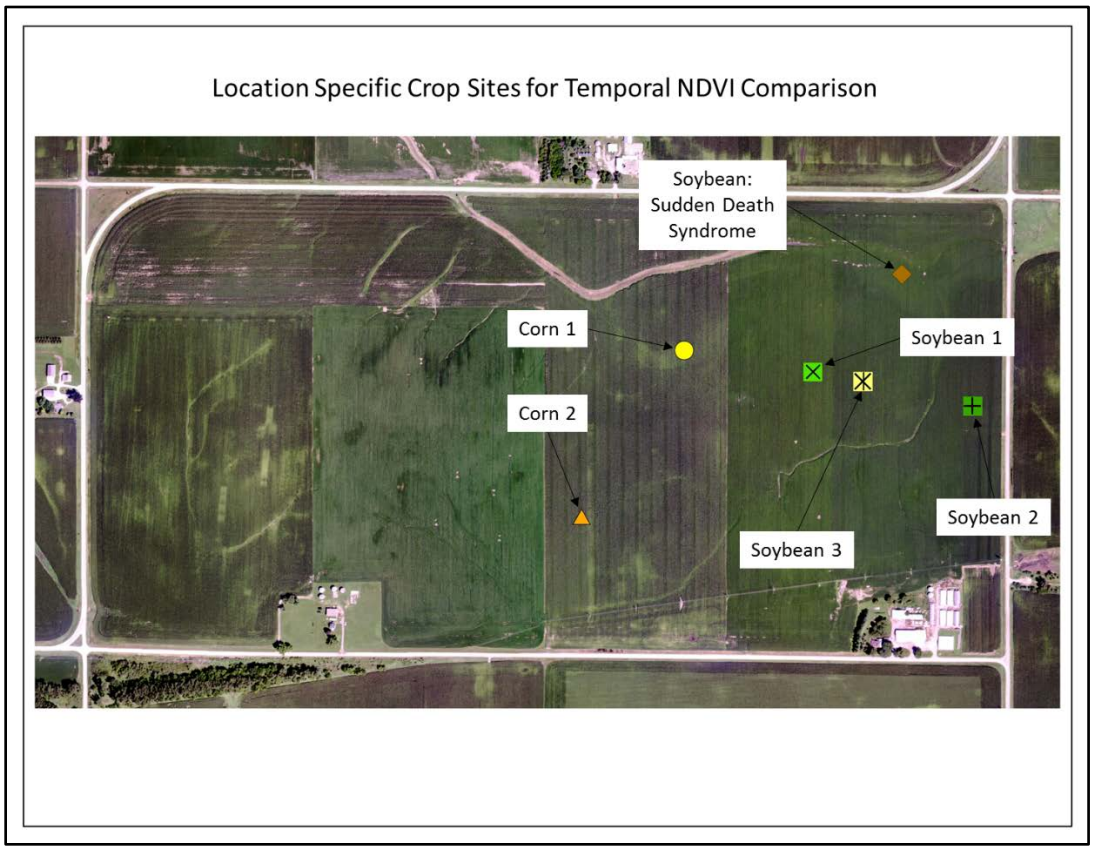

Figure 10. Random sample points in specific crop locations for temporal comparison of calibrated and uncalibrated NDVIs.

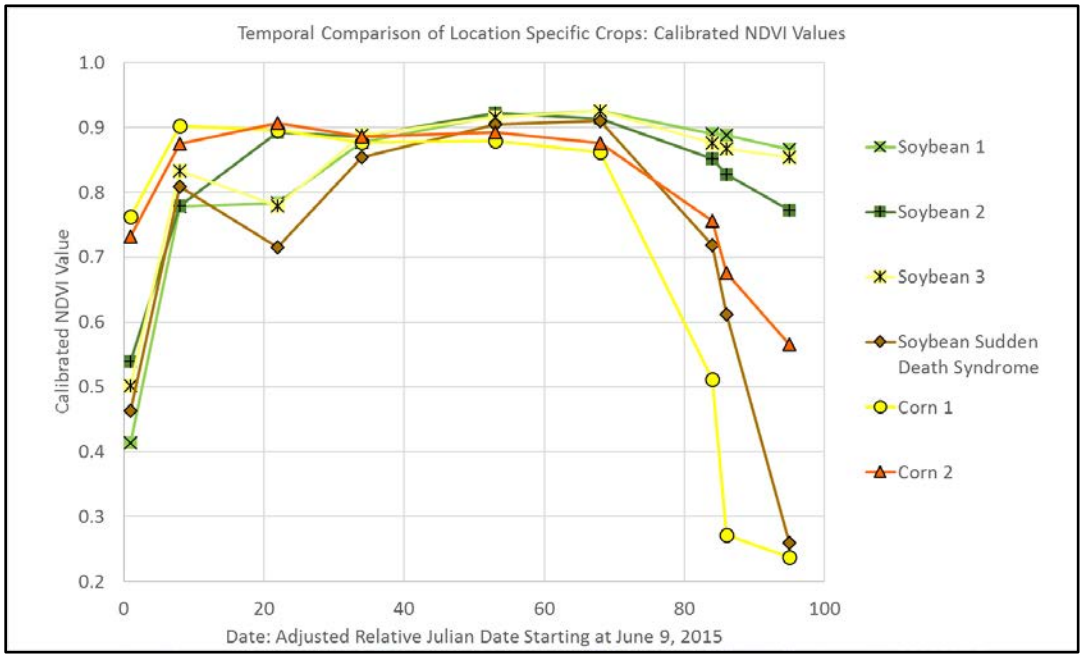

Figure 11. Calibrated NDVI values over the 2015 growing season for crop specific locations.

For comparison purposes, this study also produced an NDVI directly from the uncalibrated DNs. The result of the temporal sequences from the field points is significantly different from the calibrated and

there is no real interpretation that can be made from these graphs (Figure 12). In many ways this shows the meaninglessness of NDVI as a numeric value when the data are uncalibrated.

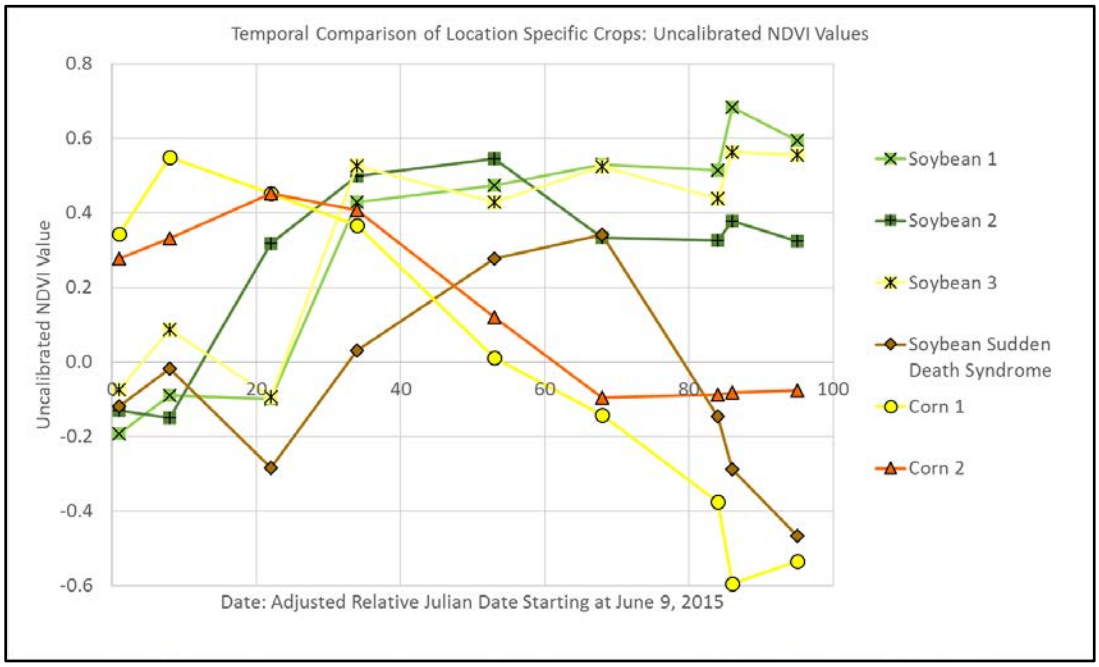

Figure 12. Uncalibrated NDVI values over the 2015 growing season for crop specific locations.

Another way of utilizing the temporal sequence of calibrated NDVI images is to apply a standardized color ramp on each image. Since the data are calibrated, the use of a standard color scheme across all images is useful for visual assessment of true change over time. From the calibrated sequence of images in Figure 13, one can see how various portions of the field change color over time from deep red, through yellow, to light green, to dark green, and ultimately back through yellow to red. This color sequence aids in seeing the effect of soil variation, grass waterways, poorly drained areas, soybean SDS, hybrid differences, residue differences, early and late senescence, and much more. When one compares the calibrated sequence of NDVIs to the uncalibrated sequence of NDVIs computed directly from DNs, there is a stark difference in their utility (Figure 14). It is interesting to note that for each of the uncalibrated images there is always almost equal amounts of all colors regardless of the time of year. For an early June image there is a great deal of deep green, which indicates healthy plants. In late July there is a great deal of yellow and red indicating very poor vegetation (even though both corn and soybean are at full canopy). While the uncalibrated images provide an insight into maximum variation across the field at any point in time, it is difficult to understand and interpret the magnitude of these differences.

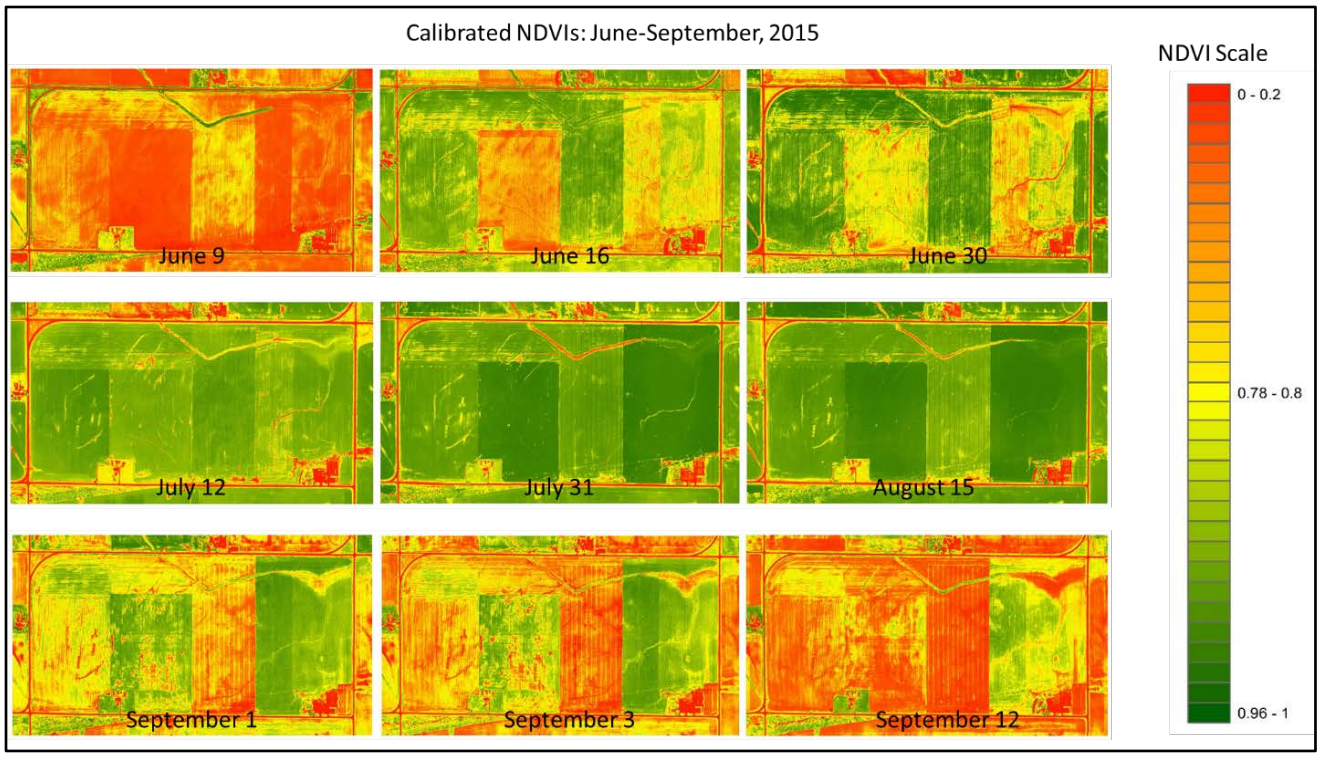

Figure 13. Temporal comparison of all nine individual calibrated NDVIs from DAI-P1 with a 32-class color scheme that maintains the same values for all colors over time.

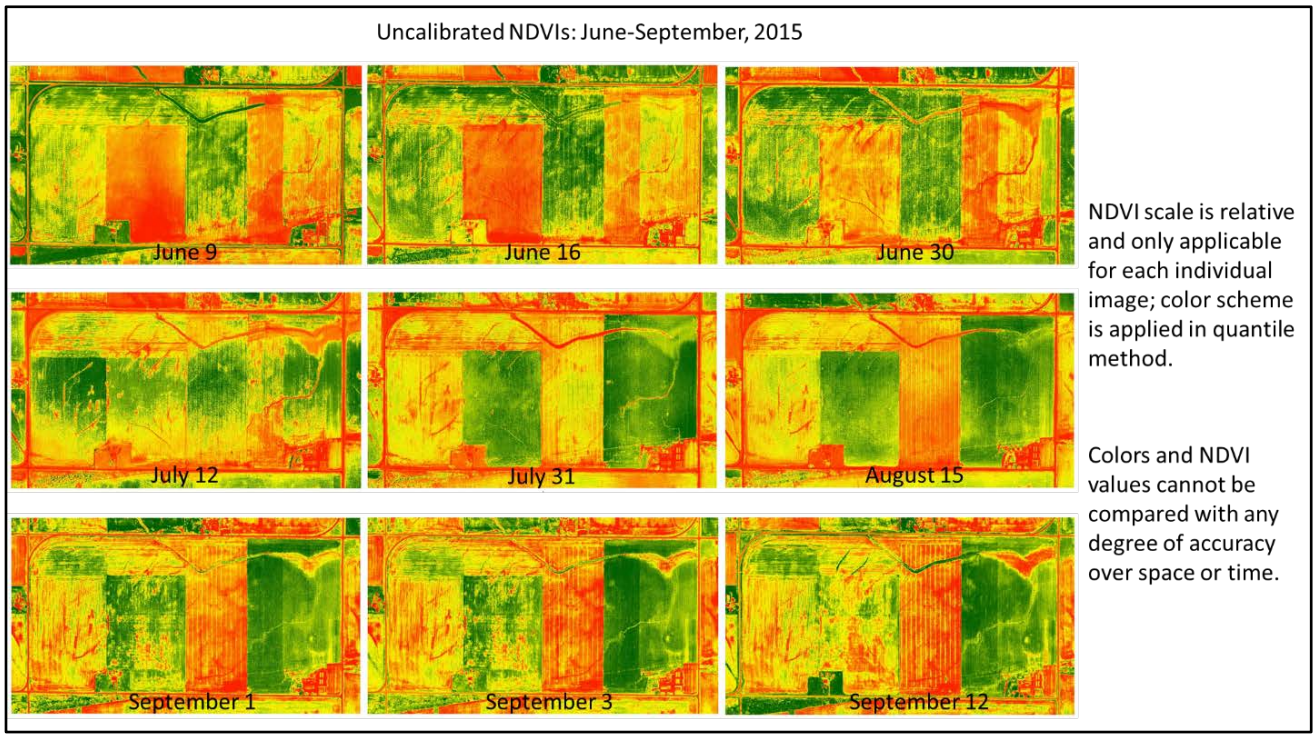

Figure 14. Temporal comparison of all nine individual uncalibrated NDVIs from DAI-P1 with the same 32-class color scheme, but the colors are scaled with quantile breakpoints.

DISCUSSION AND CONCLUSION

Throughout this preliminary research with ISA, many issues came to the forefront, but with novel approaches and sound practices, a realistic solution for radiometric calibration was attainable and produced results that were minimally variable. The beginning of building a temporal crop-health database of the remotely sensed data from the study site in Story County, Iowa has begun with the data gathered from the 2015 growing season. The process will continue with refinements of research in the future, through developmental goals that can focus on which vegetation indices to utilize and what forms of crop monitoring and management techniques that can be applied (Hatfield and Prueger, 2010). Moreover, there are still many lessons learned from this growing season that can be built on to improve calibration techniques and the provisions of quality vegetation indices.

The following will summarize the lessons learned from this study, with suggestions for further focus to develop research techniques. First, with regard to the providers of DAI, non-linear data was problematic. Without percent reflectance tarps, which covered a large range of values, confidence in calibration of non-linear data diminished. However, with linear data the use of only two or three tarps were needed to calibrate imagery with a high degree of confidence. Second, the focus on tarp reflectance variability with relation to environmental conditions and deployment standards needs to be further investigated to gain even more confidence in results. This could be accomplished by mounting the tarps to flatter and more solid surfaces, the use of calibration coefficients (Moran et al., 2001), and/or through gaining spectroradiometer readings of the tarps at or near the time of flight. Third, the data providers must make available the camera specifications and the flight parameters for all dates of data acquisition. Fourth, the issues of image to image misregistration (not elaborated on in this research) needs to be reengaged to understand if there is a better solution or these issues may be a more significant problem in future research. Fifth, more effort should be focused on the utilization of linear data to extract a more precise DN for the 2% reflectance value as opposed to the method used in this study. If one can reliably identify the 2% DN values in an image, only one mid-level reflectance tarp may be required to effectively calibrate the data (assuming the data is linear). Finally, this study has demonstrated that radiometric calibration is fundamental to the development of vegetation indices that have any true validity for quantitative comparisons across time and space. Since vegetation indices require the use of percent reflectance, the use of uncalibrated DNs to calculate NDVI or other vegetation indices will yield results that are not concurrent with the appropriate index values and will only represent the range of crop health relative to that specific time and location. In other words, producing a vegetative index without calibration will only produce results that show a range of the best and worst vegetation in a given area at a given moment.

With technology increasing in an exponential manner, the surging market of drone platforms, affordable high-quality sensors for digital image acquisition, processing software, and online applications, DAI is at the forefront of producing the data needed to aid end-users in agricultural practices to develop and implement plans that will benefit the environment, economy, and public health. Between the data providers, analysts, and end-users, the onus is now on the entire industry and management system to find ways to better utilize the potential of these technologies. Only time will tell where DAI applications and the potential of future crop management will be in the next decades. Nonetheless, the beginning of the quantitative revolution in aerial imagery is now and will only continue to become better at serving a multitude of agricultural practices moving forward.

References

Anuta, P. E. and R. B. MacDonald. 1973. Crop surveys from multiband satellite photography using digital techniques. *Remote Sensing of Environment* 2: 53-67.

Bauer, M. E., R. P Mroczynski, R. B. MacDonald, and R. M. Hoffer. 1971. Detection of southern corn leaf blight using color infrared aerial photography. In Proc. *Third Workshop on Color Aerial Photography in the Plant Sciences*. Gainesville, FL. 114-126.

Beisl, U. 2012. Reflectance calibration scheme for airborne frame camera images. *International Archives of the Photogrammetry, Remote Sensing and Spatial Information Sciences* 39: 1-7.

Clemens, S. R. 2012. Procedures for correcting digital camera imagery acquired by the AggieAir remote sensing platform. Graduate Thesis. Utah State University.

Deering, D.W. 1978. Rangeland reflectance characteristics measured by aircraft and spacecraft sensors. Ph.D. Dissertation. Texas A&M University.

Fitzgerald, G. F., D. J. Hunsaker, E. M. Barnes, T. R. Clarke, S. M. Lesch, R. Roth, and P. J. Pinter, Jr. 2003. Estimating crop water use from multispectral aerial imagery. In Proc. *Irrigation Association Conference*. Falls Church, VA. 138-148.

Gardner, B. R., Blad, B. L., Thompson, D. R., and Henderson, K. E. 1985. Evaluation and interpretation of thematic mapper ratios in equations for estimating corn growth parameters. *Remote Sensing of Environment* 18: 225-234.

Group Eight Technology (G8T). 2015a. Airborne sensor ground calibration panels: Type 822 - 3 meter, four level gray panels reflectivity - 6%, 12%, 22% & 44%. *Technical Manual* (G8T-TM-15-082-82, completed in May with accompanied raw data): 1-5.

———. 2015b. Airborne sensor ground calibration panels: Type 822 - 3 meter, two level gray panels reflectivity - 3% & 56%. *Technical Manual* (G8T-TM-15-082-103, completed in August with accompanied raw data): 1-5.

Hatfield, J. L., A. A. Gitelson, J. S. Schepers, and C. L. Walthall. 2008. Application of spectral remote sensing for agronomic decisions. *Agronomy Journal* 100(Supplement 3): 117-131.

Hatfield, J. L., and J. H. Prueger. 2010. Value of using different vegetative indices to quantify agricultural crop characteristics at different growth stages under varying management practices. Remote Sensing 2(2): 562-578.

Huete, A. R. 1988. A soil vegetation adjusted index (SAVI). *Remote Sensing of Environment* 25: 295-309.

Keegan, H. J., C. J. Schleter, W. A. Hall, and G. M. Hass. 1956. Spectrophotometric and colorimetric study of diseased and rust resisting cereal crops, National Bureau of Standards, Report 4591. NBS: Gaithersburg, MD.

Kyveryga, P. M., T. M. Blackmer, and R. Pearson. 2012. Normalization of uncalibrated late-season digital aerial imagery for evaluating corn nitrogen status. *Precision Agriculture* 13(1): 2-16.

Markelin, L., E. Honkavaara, J. Peltoniemi, E. Ahokas, R. Kuittinen, J. Hyyppä, J. Suomalainen, and A. Kukko. 2008. Radiometric calibration and characterization of large-format digital photogrammetric sensors in a test field. *Photogrammetric Engineering and Remote Sensing* 74(12): 1487-1500.

Moran, S. M., R. B. Bryant, T. R. Clarke, and J. Qi. 2001. Deployment and calibration of reference reflectance tarps for use with airborne imaging sensors. *Photogrammetric Engineering and Remote Sensing* 67(3): 273-286.

Moran, S. M., G. Fitzgerald, A. Rango, C. Walthall, E. Barnes, W. Bausch, T. Clarke et al. 2003. Sensor development and radiometric correction for agricultural applications. *Photogrammetric Engineering and Remote Sensing* 69(6): 705-718.

Oosterbaan R.J., D.P. Sharma, and K.N. Singh. 1990. Crop production and soil salinity: Evaluation of field data from India by segmented linear regression. Symposium on *Land Drainage for Salinity Control in Arid and Semi-Arid Regions*. Cairo, Egypt. 373-383.

Pearson, R., J. Grace, and G. May. 1994. Real-time airborne agricultural monitoring. *Remote Sensing of Environment* 49(3): 304-310.

Qi, J, A. Chehbouni, A. R. Huete, Y. H. Kerr, and S. Sorooshian. 1994. A modified soil adjusted vegetation index. *Remote Sensing of Environment* 48(2): 119-126.

Richardson, A.J., Everitt, J.H., and Escobar, D.E., 1991. Calibration of gain compensated aerial video digital count data using ground reflectance standards. In Proc. *Thirteenth Workshop of Color Aerial Photography and Videography in the Plant Sciences and Related Fields*. Amsterdam, Netherlands. 87-97.

Shanahan, J. F., J. S. Schepers, D. D. Francis, G. E. Varvel, W. W. Wilhelm, J. M. Tringe, M. R. Schlemmer, and D. J. Major. 2001. Use of remote sensing imagery to estimate corn grain yield. *Agronomy Journal* 93(3): 583-589.

Smith, G. M., and E. J. Milton. 1999. The use of the empirical line method to calibrate remotely sensed data to reflectance. *International Journal of Remote Sensing* 20(13): 2653-2662.

Tucker, C.J. 1979. Red and photographic infrared linear combinations for monitoring vegetation. *Remote Sensing Environment* 8(2):127-150.

Zhang, H., Y. Lan, R. Lacey, W. C. Hoffmann, and Y. Huang. 2009. Analysis of vegetation indices derived from aerial multispectral and ground hyperspectral data. *International Journal of Agricultural and Biological Engineering* 2(3): 33-40.